GPR17 AND GPR52 ARE ACTIVATED BY THE ARTIFICIAL SWEETENERS SUCRALOSE AND SACCHARIN

BY

NICHOLAS R. FERNANDEZ

A thesis submitted to the
Department of Chemistry & Biochemistry
Mount Allison University
in partial fulfillment of the requirements for the
Bachelor of Science degree with Honours
Or Honours certificate in Biochemistry

April 22nd, 2020

Table of Contents

Abstract

G-protein coupled receptors (GPCRs) are a class of transmembrane proteins which are responsible for communication and signalling in a wide variety of cell-cell and cell-environment interactions. They are responsible for senses including smell, sight and taste, in addition to internal metabolite sensing. GPCRs are excellent drug targets due to the important role they play in a variety of physiological processes; over 34% of all FDA approved drugs target GPCRs. Orphan GPCRs are a subset of approximately 90 GPCRs which do not have an established endogenous or exogenous ligand. Artificial sweeteners are a family of organic compounds which activate the GPCR taste receptor (T1R2/T1R3) but are not metabolized by the human body leading to the initial belief that they are safe and effective sugar replacements which reduce caloric consumption. However, recent findings suggest that chronic artificial sweetener consumption may lead to glucose intolerance and metabolic disease and that unknown receptors beyond T1R2/T1R3 are capable of sensing sweet molecules. In this study, 72 family A orphan GPCRs were screened for activation through treatment with a combination of the artificial sweeteners sucralose and saccharin using the PRESTO-Tango resource for GPCR interrogation. The strength of activation in identified receptor candidates was investigated further with both natural and artificial sweeteners. Two receptors were found to be significantly activated by the artificial sweeteners, GPR17 and GPR52, which is the first report of this receptor-agonist pairing. Dose response curves revealed that artificial sweetener activated GPR17 signalling was saturated at a concentration of 2 mM with a 1.5-fold change response for saccharin and a 1.6-fold change response for sucralose relative to control. GPR17 activation was higher for the sucrose treatment with a fold change of 2.1. Conversely, GPR52 responded more strongly to artificial sweeteners with a greater than 5-fold change in receptor activation when treated by sucralose or saccharin but was not activated by sucrose. These findings suggest that these orphan receptors may play a wider role in human metabolism than has been previously considered.

Acknowledgements

I wish to express my sincere gratitude to Dr. Jillian Rourke for her guidance and mentorship throughout the last two years and especially through the course of this project. Additionally, I would like to extend my thanks to Dr. Amanda Cockshutt, my second reader. I would also like to thank all of the other students in the Rourke lab: Rachel McDougall, Madeline Power, Madelaine Russel and Brandon MacKinnon, for their collaboration and support. This project would not have been possible without generously shared lab space and equipment of Dr. Tyson MacCormack, Dr. Jeffery Waller and Mr. Tyler Lutes of Souricimed. And finally, my friends and family who were there listening to me talk at length about my project, greet me after late nights in lab and provide support at every step of the way.

The Rourke lab receives funding from NBIF and NSCERC. This project was started in Summer 2019 under an NBHRF summer studentship and was presented at the 11th NB Health Research Conference in November 2019 where it received a 3rd place poster award.

Introduction

1. G-Protein Coupled Receptors

G-protein-coupled receptors (GPCRs) are a large family of membrane receptors responsible for mediating many physiological functions including metabolism, smell and taste (Rosenbaum et al., 2009). Many GPCRS serve as promising drug targets; over one-third of all drugs currently approved by the FDA act against GPCRs (Hauser et al., 2017). There are over 800 GPCRs which have been classified within the human genome, of which approximately 300 are categorized as non-olfactory rhodopsin and glutamate family receptors (Jassal et al., 2010; Lv et al., 2016). These GPCRs provide the basis for regulating homeostasis through recognition of endogenous, exogenous and synthetic compounds (Husted et al., 2017; Shioda et al., 2008). Dysfunction in GPCR signalling has been linked to a number of health problems, including cancer, immune disorders and metabolic diseases such as diabetes and obesity (Husted et al., 2017).

1.1 GPCR Structure

Although GPCRs are responsible for sensing a wide variety of molecules, including proteins, sugars, lipids and even light, GPCR structure is highly conserved across families of these receptors. In all GPCRs, the hydrophilic N-terminal end of the receptor is located in the extracellular matrix with a diversity of conformations and lengths depending on the GPCR family (Kobilka, 2007). GPCRs are divided into 5 families: rhodopsin (family A), secretin (family B), glutamate (family C), adhesion and frizzled (family F). Families are classified by both the chemical nature of their ligands and the structure of their N-terminal domain (Rosenbaum et al., 2009). Of these, families A and C are considered to be among the most common. Rhodopsin-like receptors (family A) constitute the largest of these families and are named for their similarity to the photon-sensing rhodopsin receptor, a GPCR responsible for vision found in retinal cells. Family A receptors are also responsible for sensing a variety of organic molecules including small peptides, nucleic acids, glycoprotein hormones and chemokines (Harmar, 2001). Family A GPCRs do not have large extracellular domains but instead have a binding pocket with both hydrophobic and hydrophilic residues

located within the seven transmembrane helices (Kobilka, 2007). Conversely, family C receptors are responsible for sensing molecules like calcium, umami and sweet tastants, among other metabolites (Harmar, 2001; Husted et al., 2017). This family is distinguished from family A receptors by large N-terminal domains and receptor pairing through dimer formation with other GPCRs. For example, both the umami and sweet taste receptors are comprised of different combinations of three family C GPCRs: T1R1, T1R2 and T1R3. The umami receptor is assembled from T1R1 and T1R2, while the sweet taste receptor is made from T1R2 and T1R3. This combination of receptors allows for allosteric modification of receptor activity through protein-protein interactions and modified signalling through the pair of C-terminal domains (Sanematsu et al., 2014a). Much of the core sequence of the family C receptor remains the same as family A receptors. For example, allosteric modulators of family C GPCRs bind in the hydrophobic transmembrane pocket within or between receptor dimers (Gurevich and Gurevich, 2019).

All GPCRs have a series of hydrophobic alpha helices which pass through the cellular membrane seven times, regardless of the family to which they belong. This feature is critical to the identification of putative GPCRs throughout the human genome, as a set of seven sequences of 10 to 20 hydrophobic amino acids indicates the presence of a GPCR regardless of whether the receptor has been physiologically characterized (Kobilka, 2007). This leads to a situation where GPCRs may be predicted by amino acid sequence but exist without known functions or ligands (see section 1.3 Orphan GPCRs). At the C-terminal end, GPCRs have a cytosolic domain which associates with a heterotrimeric G-protein. The latter dissociates and acts as a signalling effector upon GPCR activation.

1.2 GPCR Function

GPCR function is directly related to protein structure and relies on conformational changes in response to extracellular ligand binding which propagate signals through the membrane to activate the heterotrimeric G-protein ($G\alpha\beta\gamma$). The $G\alpha$ subunits of these heterotrimeric G proteins fall into four main families, G_i, G_q, G_s and G_{12}, in addition to specialized isoforms such as $G_{gustducin}$ which are associated with unique processes

including taste (Latek et al., 2012). Each family of Gα proteins is associated with a cellular response, typically through a common signal transduction effector. For example, the sweet taste receptors signal mainly through the G_s pathway, which increases cytoplasmic concentration of cyclic AMP (cAMP) through the activation of adenylyl cyclase (AC). In contrast, a subset of inhibitory GPCRs signal through G_i, which decreases levels of cAMP (McCudden et al., 2005). These effectors initiate signal transduction cascades where the message communicated by a single receptor is amplified each time it passes to a new effector, which may produce a greater than ten thousand-fold molecular response in a short period of time. While much of the attention surrounding GPCR signalling is focused on Gα, the Gβγ has long been known to play a central role in the function of GPCRs. A variety of subtypes for each Gβγ subunit are used to regulate signalling to a greater extent than Gα could alone. As Gβγ does not contain a catalytic domain, its function is restricted to regulation of other signalling molecules, including phospholipase C (PLC), AC, Raf and Ras, through protein-protein interactions. It also plays a key role in the recruitment of GPCR kinases which phosphorylate the C-terminal domains of activated GPCRs (Smrcka, 2008). The phosphorylated C-terminal domain then recruits β-arrestin, a regulatory protein which terminates signalling and promotes internalization of the receptor. Once internalized the GPCR may be degraded or reactivated through dephosphorylation and recycled back to the membrane.

While some GPCRs are conserved among cell or tissues types, driving ubiquitous cellular processes like survival and propagation, others are unique and serve specialized purposes. GPCRs fill a wide variety of roles important to homeostasis and respond to a diverse array of signals, making them prime candidates for drug targeting in the treatment of many diseases (Hauser et al., 2017). However, only a small proportion of the entire family have approved drugs which modulate their activity and more investigation is required to fully utilize GPCRs in the field of medicine (Hauser et al., 2017).

1.3 Orphan GPCRs

Not all GPCRs found within the human genome have a known endogenous ligand. Despite several decades of specific targeting through the process of deorphanization as ligands are discovered for these receptors through high throughput screening and molecular modelling this approximately 90-member family of orphan GPCRs remains (Fang et al., 2015).

A majority of these orphan receptors, over 72, belong to family A and are of particular interest to sensing sweet molecules due to the large role that deorphanized members of this family have in metabolism (Husted et al., 2017).

Constitutively active receptors, GPCRs which do not require a ligand to generate a signal transduction cascade, are a common type of orphan receptor. Despite not requiring ligands for signalling, the quantity and quality of the message communicated by constitutively active GPCRs can be drastically changed by allosteric modulators (Tao, 2008). Due to the many roles that GPCRs play in physiology, orphan receptors are of great interest as a previously uninvestigated set of drug targets (Fang et al., 2015). However, even if a receptor does not have a known endogenous ligand, it still may be implicated in characterized processes both directly and indirectly. Quantitative expression profiling of a number of diseases states including cancer, obesity and diabetes have linked changes in orphan GPCR surface expression to pathogenesis (Morri et al., 2018). Receptor deorphanization has also been used to better characterize physiological processes. Deorphanization of GPCRs in the brain has led to better understanding of how GPCR signalling contributes to sleep/wake cycles and puberty across the previous 30 years (Civelli, 2012). Many orphan GPCRs are not only found in humans but other animals as well. Evolutionarily, Gα proteins are conserved across metazoa and beyond, with many receptors responding to identical ligands shared across many mammalian species (Hu et al., 2017; de Mendoza et al., 2014). Therefore, greater understanding of orphan receptors furthers comprehension of fundamental biological processes for not only humans, but all eukaryotic life.

2. Physiological Response to Sugars

2.1 Overview of Sweet Taste Receptors

The main GPCRs responsible for the transduction of sweet taste form a heterodimer composed by the two class C GPCRs, T1R2 and T1R3. T1R2/T1R3 senses a variety of sweet molecules with diversity of origin and structure, including mono- and di-saccharides like glucose and fructose, artificial sweeteners like sucralose and saccharin, sweet amino acids including *D*-tryptophan and *D*-phenylalanine and even sweet proteins (Lee and Owyang, 2017).

2.2 Sweetener Sensing in the Tongue

The sweet taste receptor T1R2/T1R3 plays a major role in the overall response of the human body to sweet molecules. Type II taste cells, which are found in taste buds, express T1R2/T1R3 and serve as the first point of sweet molecule detection in the GI tract (Laffitte et al., 2014). Through GPCR signalling processes associated with Gα-gustducin, the receptor is able to induce membrane depolarization through activation of the potassium channel TRPM5 and stimulate release of ATP, a neurotransmitter which acts on primary gustatory neurons to communicate the signal to the brain (Laffitte et al., 2014). T1R2/T1R3 is likely not the only mechanism of glucosensing in the tongue; type II taste cells also express the active and passive glucose transporters SGLT-1 and GLUT-2, which suggests that there are mechanisms of sensing glucose concentrations in the cytoplasm (Merigo et al., 2011). Studies have also shown that taste cell sensitivity to sweet molecules, and perception of satiety when consuming sweet foods, is regulated by the hormone GLP-1. Knockout murine models of GLP-1 demonstrate a significant reduction in sensitivity to sweet (and umami) tastants. Additionally, GLP-1 degrading enzymes are downregulated in type II taste cells, allowing higher concentrations of the hormone to persist for longer periods of time (Martin et al., 2009). Together, these findings suggest that GLP-1, and paracrine signalling in general, is integral to high sensitivity glucosensing in taste buds.

2.3 Sweetener Sensing in the Gastrointestinal (GI) System

Beyond the tongue, glucosensing is common to cells throughout the small intestine including enterocytes, enteroendocrine cells (EECs) and enteric neurons. Enterocytes make up the largest population of sugar-sensitive cells within the small intestine and are responsible for the majority of glucose uptake from the GI tract into the circulation (Fournel et al., 2016). SGLT-1, a sodium-glucose symporter found on the apical membrane of enterocytes, transports glucose from the lumen into the cytosol where it then exits through the basolateral membrane *via* passive facilitated diffusion through GLUT-2 (Wright et al., 2003). EECs are also connected to circulation through the apical and basolateral membranes, but their primary role is paracrine and endocrine signalling through the release of hormones like GLP-1 and GIP. In these polarized cells, entry of glucose through SGLT-1 opens Ca^{2+} channels to induce membrane depolarization and vesicle release (Depoortere, 2014). While the effects of these hormones are systemic, enteric neurons located within the epithelium express GLP-1 receptors in close proximity to EECs allowing communication through the gut-brain axis with the hypothalamus, the area of the brain responsible for metabolism and appetite (Leloup et al., 2016). Additionally, enteric neurons may be able to respond to glucose directly through elevation of cytoplasmic stores *via* SGLT-3, allowing activation of proximal neurons as well as direct communication with the brain (Díez-Sampedro et al., 2003).

2.4 Sweetener Sensing in the Pancreas

A major target of the GLP-1 and GIP produced by EECs is the pancreas. Particularly, β-cells found in the islets of Langerhans are responsible for the detection and management of elevated levels of plasma glucose. Similar to other glucosensing cells, β-cells transport glucose into their cytoplasm through GLUT-2. β-cells contain the specialized isoform hexokinase IV, which phosphorylates glucose to prevent efflux from the cell. Increases in plasma glucose induce expression of hexokinase IV. Therefore, as blood glucose rises and cellular respiration flux increases, ATP accumulates in the cytoplasm of β-cells. This inactivates K_{ATP} channels, depolarizing the membrane and releasing insulin (MacDonald et al., 2005; Schuit et al., 2001). In this way, sugars are

directly responsible for insulin secretion. Insulin is responsible for initiating a number of systemic effects to decrease levels of circulating glucose. Insulin promotes translocation of GLUT-4 to the cell surface in many cell types, which allows glucose uptake from the blood, activates hexokinase and 6-phosphofructokinase to increase flux through glycolysis and promotes glycogen synthesis in muscle and liver to develop stores of glucose for released during fasting (Saltiel and Kahn, 2001). Direct sensing of glucose is not the only mechanism that can stimulate insulin secretion. β-cells also respond directly to GLP-1 secretions from EECs through GLP-1 receptors, leading to release of insulin stores (MacDonald et al., 2002). Studies have shown that co-activation of these receptors with increases in circulating glucose are required for maximal secretion of insulin. Injections of glucose elicit one third of the insulin secretion response observed with oral glucose consumption due to the release of the incretins, GLP-1 and GIP, by enteroendocrine cells (Holst, 2007). This emphasizes the importance of surface level sweet molecule sensing by both the taste buds and enteroendocrine cells within the GI system.

2.5 Sweetener Sensing in the Brain

The role of the hypothalamus in sensing and coordinating glucose metabolism through the gut-brain axis and autonomous nervous system (ANS) is the final element required to understand glucosensing. Once enteric neurons are activated by EECs, the signal is delivered to the brain stem through neuronal signaling which then stimulates GLP-1. GLP-1 then reaches the hypothalamus where catecholamines are released to stimulate the ANS, permeating peripheral tissues to improve insulin sensitivity (Knauf et al., 2008). Through this multi-organ effort, the detection of glucose prepares the human body to both expend and store incoming sources of energy. Signalling processes are tied to both the extracellular and intracellular sensation of sweet molecules, which were traditionally thought to be exclusively natural sugars but now prove to be activated by a number of artificial sweeteners with a great variety of potential consequences for metabolism and health.

3. Artificial Sweeteners

Artificial sweeteners, a class of increasingly popular food additives, are useful as a replacement for conventional sugar because they are both far sweeter than natural sugars and are not metabolized by the body, and therefore do not contribute directly to caloric intake (Table 1). However, this does not mean that they do not contribute to metabolic changes within the body as had been initially believed. Artificial sweeteners lead to a variety of systemic disturbances due to activation of the sweet taste receptor and the effects described above without the body's expected increase in blood glucose or energy state.

Table 1: Structures, origins and perceived sweetness of common natural and artificial sweeteners. Relative sweetness is listed in comparison with sucrose activation of the sweet taste receptor, T1R2/T1R3 (Magnuson et al., 2016).

Structure	Information
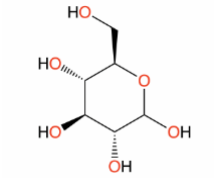	**Glucose** Natural monosaccharide Relative Sweetness: 0.56
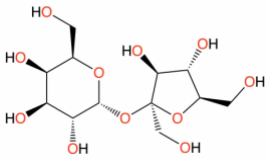	**Sucrose** Natural disaccharide Relative Sweetness: 1
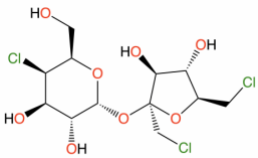	**Sucralose** Artificial Sweetener Relative Sweetness: 600
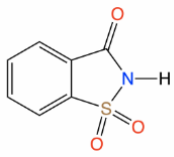	**Saccharin** Artificial Sweetener Relative Sweetness: 300

3.1 Sucralose

Sucralose is a common artificial sweetener, structurally identical to sucrose but with chlorine functional groups replacing 3 hydroxyl groups. Sucralose is not metabolized following consumption and very little is absorbed from the GI tract. The low

proportion which enters the blood stream is cleared quickly by the kidney Chattopadhyay et al., 2014). Sucralose is more than 600 times sweeter than sucrose when sensed by the sweet taste receptor, and has a greater than two-fold increase in potency with an EC50 of approximately 27 µM in comparison to 60 µM for sucrose (Shimizu et al., 2014; Zhang et al., 2010). Consumption of sucralose increases the epithelial expression of the active glucose transporter SGLT-1, in addition to systemic increases in the hormone GLP-1 (Geraedts et al., 2011). This suggests that sucralose is not only recognized throughout the GI tract but is also capable of producing systemic responses to glucose through processes including insulin secretion.

3.2 Saccharin

Saccharin is composed of a functionalized benzene ring, more specifically 1,2-benzoisothiazol-3-(2H) on a 1,1 dioxide. In contrast to sucralose, most of the saccharin consumed by a given host is able to freely enter the body and diffuse quickly through the plasma through reversible protein binding (Magnuson et al., 2016). Saccharin is also rapidly cleared by the renal system with a half-life of less than 70 minutes when delivered by intravenous injection (Sweatman et al., 1981). Early work definitively established that saccharin is not metabolised by the body, even as it permeates both blood and tissue (Renwick, 1985). While previous studies have linked chronic saccharin consumption to bladder cancer in animal models, no study has established a cancer link in humans and the sweetener is still considered safe (Chattopadhyay et al., 2014). Saccharin remains in use in small amounts or in combination with other sweeteners due to its bitter after-taste at higher concentrations (Chattopadhyay et al., 2014). Saccharin is 300 times sweeter than an equivalent mass of sucrose but has a lesser potency of 300 µM (Sanematsu et al., 2014).

3.3 Mechanisms of Artificial Sweetener Mediated Disturbances

Recent *in vitro* models in human embryonic kidney (HEK293) cells of artificial sweetener toxicity, quantified by MTT assay, suggest that sucralose and saccharin induce sweetener-dependent DNA damage (van Eyk, 2015). However, the concentrations and durations of exposure, 1 mM across 72 hours, described in the

experiment are not physiologically relevant to products currently available on the market. This work provides rationale for more concrete investigation of artificial sweeteners and their influence on macromolecules in the cell.

In addition to their effects on human cells, artificial sweeteners may also exhibit their effects on the gut microbiome. In model *E. coli*, both sucralose and saccharin inhibit growth and cause cytotoxicity (Harpaz et al., 2018). This provides a second rationale of further investigating artificial sweeteners in an era with greater “omic” power and ability to investigate the patterns and interaction of bacteria that constitute the gut microbiome. Several studies in rats have demonstrated that chronic consumption of artificial sweeteners significantly decreases populations of beneficial anaerobic bacteria within the gut microbiome including *Bifidobacterium*, *Lactobacillus*, and *Bacteriodes.* As of now there is insufficient evidence to know the mechanism by which artificial sweeteners impact gut microbiota including possibly inhibiting growth of these bacteria or promoting the growth of their competitors (Abou-Donia et al., 2008). In mice, chronic artificial sweetener consumption is positively associated with glucose intolerance, a condition which can lead to type 2 diabetes. Glucose intolerance was transferred by fecal transplantation into germ-free mice, confirming that the changes originated in the microbiome (Suez et al., 2014).

Beyond the microbiome, artificial sweeteners are also able to change human metabolism directly. As described above, artificial sweeteners are able to signal through the same mechanisms as natural sweeteners without the associated increase in calories. Saccharin-stimulated adipogenesis clearly demonstrates how these effects influence systemic energy homeostasis. While organism-wide energy status is often communicated through hormonal (insulin) and paracrine (adipokine) signalling in adipose tissue, many differentiated and pre-differentiated adipose cells are also able to sense sweeteners directly through T1R2/T1R3 and other receptors. Recent *in vitro* work in partially differentiated adipose cells has demonstrated that while saccharin is not required for differentiation to mature adipocytes, the sweetener stimulates the process through a mechanism independent of T1R2/T1R3 and reliant on phosphorylation of the common transduction effector Akt (Simon et al., 2013). Saccharin was also shown to inhibit the release of energy stores through lipolysis, again in a manner independent of

T1R2/T1R3. These findings suggest that there are additional receptor(s) responsible for sensing sweet molecules, and that artificial sweeteners are capable of directly exerting effects which can contribute to metabolic disease. Given that artificial sweeteners activate known GPCRs, it is likely that the unknown receptors which are activated by sweet molecules are also GPCRs. The family A GPCRs, in particular, are commonly involved in responses to food metabolites and regulation of energy homeostasis (Husted et al., 2017). Additionally, there are over 72 family A orphan receptors, which presents a large number of potential targets.

5. Experimental Objectives

While some of the physiological and pathological changes associated with artificial sweetener consumption are known, the mechanisms by which they affect the body are still not fully characterized. Type 1 taste receptor signalling is also not fully understood and may play a substantial role in the metabolic effects associated with chronic artificial sweetener consumption. We hypothesize that some orphan GPCRs, especially those in the metabolically active rhodopsin family (family A), may play a role in the metabolic effects associated with chronic artificial sweetener consumption based on expression profiles and the receptor families known to be involved in metabolite sensing. In this experiment, we measured the activity of 72 orphan GPCRs in response to treatment with the artificial sweeteners sucralose and saccharin using a GPCR proximity assay. The Parallel Receptor-ome Expression and Screening via Transcriptional Output - Transcriptional activation following arrestin translocation (PRESTO-Tango) assay is an open-source platform for conducting entire GPCR-ome screening (Barnea et al., 2008; Kroeze et al., 2015). The system takes advantage of stably transformed luciferase and an isoform of β-arrestin conjugated to TEV protease in the HEK-derived HTLA cell line. When receptors are activated, they are phosphorylated and then recruit β-arrestin. In the PRESTO-Tango system, the protease associated with β-arrestin cleaves a transcription factor (TF) on the C-terminus end of the GPCR allowing the TF to translocate to the nucleus and initiate expression of luciferase. Luciferase oxidation of *D*-luciferin produces light proportionally to GPCR activation, which can be measured through a luminescence detector. The resource contains 315 GPCRs, 72 of which are

family A orphan receptors. However, due to the near ubiquitous nature of β-arrestin of GPCRs in signal termination, PRESTO-Tango may provide information about receptor activation even if little is known about the receptor (Kroeze et al., 2015). Therefore, we hypothesize that it may be a useful platform in the pursuit of deorphanization particularly for generic ligands such as metabolites and sweeteners. Validation experiments will be conducted to determine which of the artificial sweeteners is responsible for the activation of each chosen receptor. Once orphan receptors activated by the combination of sweeteners have been identified, dose response curves will be used to quantify EC50 for the validated receptors with both natural and artificial sweeteners. These studies are important because little is known about the biological basis of artificial sweetener sensing, particularly as it relates to adipogenesis, dysregulation of glucose sensing and metabolic disease beyond the sweet taste receptor. Improved understanding of sweet molecule sensing at a molecular level will help not only in clarifying what the full effects of chronic artificial sweetener consumption might be, but also in developing and categorizing new artificial sweeteners which may not exhibit the same effects.

Methods

1. Plasmids Preparation

PRESTO-Tango plasmids were obtained from an AddGene depository created by Dr. Bryan Roth (Kroeze et al., 2015). pBluescript II SK(+) and pCMV-β-galactosidase reference plasmid were also used as empty vectors and transfection efficiency controls, respectively. Transformed *E. coli* were cultured on LB agar (BioShop; LBL508.500) with 50 µg/mL ampicillin overnight at 37° before inoculation in LB broth (BioShop; LBL407.500) with 50 µg/mL ampicillin and grown overnight at 37° with oscillation at 180 rpm. Plasmid purification was completed according to the protocol for isolation of transfection-grade plasmid DNA in low throughput with NucleoSpin Plasmid Transfection-grade kit (Machery-Nagel; 740490.250).

2. Cell Culture

HEK293-derived HTLA cells, developed by Barnea *et al.* (2008), were grown at 37° and 5% CO_2 in high glucose DMEM (VWR; CA45000-304) with 10% FBS (VWR; 97068-085), 2 µg/ml puromycin (Bioshop; PUR333.100) and 100 µg/ml hygromycin B (Bioshop; YG002.1).

4. Toxicity Curves

HTLA cells were plated at 25,000 cells/well in high-glucose DMEM with 1% FBS in 96-well format at 37°C with 5% CO_2. At 24 hours post-plating, 70% of plating media was exchanged with OptiMEM. Cells were incubated for an additional 24 hours and media was partially exchanged with OptiMEM containing the artificial sweeteners across the range of doses. Cells were incubated for 24 hours before 3-(4,5-Dimethylthiazol-2-yl)-2,5-Diphenyltetrazolium Bromide (MTT);(Bioshop; MTT222.500) was added to each well to a final concentration of 0.05 mg/mL and incubated for 2.5 hours at 37°C. Media was gently removed from each well and the remaining formazan crystals were resuspended in DMSO (Bioshop; DMS555.500) by oscillating for 15 minutes while protected from light. Absorbance at 570 nm was read with a SpectraMax microplate spectrophotometer. This experiment was completed with two biological replicates.

4. PRESTO-Tango Luciferase Assay

4.1 Plating

HTLA cells were plated at 25,000 cells/well in 100 µL high-glucose DMEM with 5% fetal bovine serum (FBS) in 96-well format (Grenier; 650160) at 37°C with 5% CO_2. All culture plates were grown under the culture conditions described above and harvested at confluences of less than 60%.

4.2 Transfection

At 24 hours post-plating cells were transfected with a subset of 25 ng LPAR-Tango constructs (AddGene, 1000000068), 25 ng pCMV-βGal and 50 ng pBSK with 200 ng polyethylenimine (PEI) in OptiMEM (Fisher, 31985070). PEI and each of the DNA vectors were combined with gentle agitation and incubated for 15 minutes at room temperature before being applied to the cells through media exchange.

4.3 Treatment

Cells were incubated for 24 hours following transfection and media was partially replaced with OptiMEM (vehicle) alone or FBS and artificial sweetener (treatment) in OptiMEM, depending on the experiment.

4.4 Lysis

Cells were incubated for 24 hours following treatment before media was removed and cells were lysed with luciferase lysis buffer (Biotium; 99923) and frozen at -80°C for a minimum of 24 hours. Cell lysate was thawed and diluted 1:9 with MiliQ H_2O before immediately proceeding to β-galactosidase and luciferase assays.

4.5 β-Galactosidase Assay

Transfection efficiency was quantified through a β-Galactosidase assay. Lysate was combined in a 1:1 ratio with β-Galtosidase assay buffer containing 1.33 mg/mL ONPG (VWR; 97062-374) and incubated for 5 minutes before absorbance was measured at 420 nm (A420) with a SpectraMax microplate spectrophotometer (VWR; CA89429-536).

4.6 Luciferase Assay

D-luciferin (Biotium; 30028) was added to the lysate in a 1:2 ratio and incubated with shaking for 5 minutes at room temperature before measuring luminescence with a BioTek Syngergy HT multi-detection microplate reader. Relative luminescent units (RLU) were taken as the quotient of the luminescence over A420. Data analysis and plotting was conducted in RStudio. Except where noted, experiments have been conducted with three biological replicates and three technical replicates for each transfection and treatment condition.

5. Luciferase Optimization

Luciferase optimization followed the general procedure outlined in section 4, PRESTO-Tango luciferase assay. Cells were plated under the conditions described above while varying the confluence that cells were harvested at, the concentration that cells were plated at and concentration of FBS in culture media. At 24 hours post-plating cells were transfected with the LPAR-Tango vector. Following another 24-hour incubation, cells were treated with either OptiMEM (vehicle) or 10% FBS. No changes were made to lysis or assay protocols. This experiment was completed with two biological replicates.

6. Orphan Receptor Screen

The orphan receptor screen followed the general procedure outlined in section 4. At 24 hours post-plating, cells were transfected with 72 family A orphan Tango vectors. Following another 24-hour incubation, cells were treated with either OptiMEM (vehicle) alone or a combination of 1 mM saccharin and 300 µM sucralose in OptiMEM (treatment). No changes were made to lysis or assay protocols.

7. Orphan Receptor Validation

The procedure for receptor validation replicated the process described in section 4 with minor deviations. At 16 hours post-plating, cells were transfected with GPR17 or GPR52 Tango vectors. Cells were then incubated for 24 hours and media was partially replaced with OptiMEM (vehicle) alone or 1 mM saccharin and 300 µM sucralose both alone and in combination. No changes were made to lysis or assay protocols.

8. Dose Response Curves

The procedure for artificial sweetener dose response curves replicated the process described in section 4 with minor deviations. At 16 hours post-plating, cells were transfected with GPR17 or GPR52 Tango vectors. Cells were then incubated for 24 hours and media was partially replaced with OptiMEM (vehicle), or sucralose, saccharin or sucrose over a range of concentrations from 0.01 mM to 8 mM. No changes were made to lysis or assay protocols. This experiment was conducted for only one biological replicate.

9. Statistics and Visualization

Data visualization was completed in RStudio for all figures using the ggplot2 package (Wickham, 2009). Likewise, statistics were completed in RStudio for both the orphan receptor screen and the orphan validation experiments. For both experiments, Shapiro and Barlett's tests were used to determine normality and homogeneity of variances, respectively, with a significance level set at $p = 0.05$. Orphan receptor screen data which met the standard for parametricity was compared using a student's t-test while data which was not parametric was compared using the Wilcoxon signed-rank test, again with $p = 0.05$. Receptors which met this threshold were selected for future study and validation of activation response. Orphan receptor validation data was compared using a one-way ANOVA with significance level set at $p = 0.05$.

Results

Luciferase optimization experiments were conducted with LPAR1 from the PRESTO-Tango system in order to obtain conditions which generate a response robust enough to consistently give a z-score metric for high throughput screening of greater than 0 in order to reduce the quantity of false positives obtained. Cells harvested at 50% confluence and lower on the day of plating demonstrated higher transfection efficiency as quantified by GFP and β-galactosidase assays, healthier morphology and higher luciferase expression than those harvested at high densities (Figure 1, Panel A). Cells plated below concentrations of 25,000 cells/well had greater relative luminescence unit (RLU) values in comparison to those above, to a maximum 12.9-fold change at 10,000 cells/well. Cell plating concentrations below 25,000 cells/well also had greater variability than the chosen plating concentration, with SEM values of more than double. (Figure 1, Panel B). Finally, both 5% and 10% FBS demonstrated increases in RLU relative to cells plated with 1% FBS. 250% and 300% increases in receptor activation were observed for the 5% FBS and 10% FBS conditions, respectively. There was less variability in LPAR1 activity for cells plated with 5% FBS relative to the 10% FBS condition, with a reduction to 29% of the SEM value for fold change of the 10% treatment (Figure 1, Panel C). Directed by these findings, optimization of cell plating density (25000 cells/well), cell confluence at the time of plating (< 50%) and concentration of serum at time of plating (5%), resulted in a Z score of 0.27. (Figure 1; Panel D).

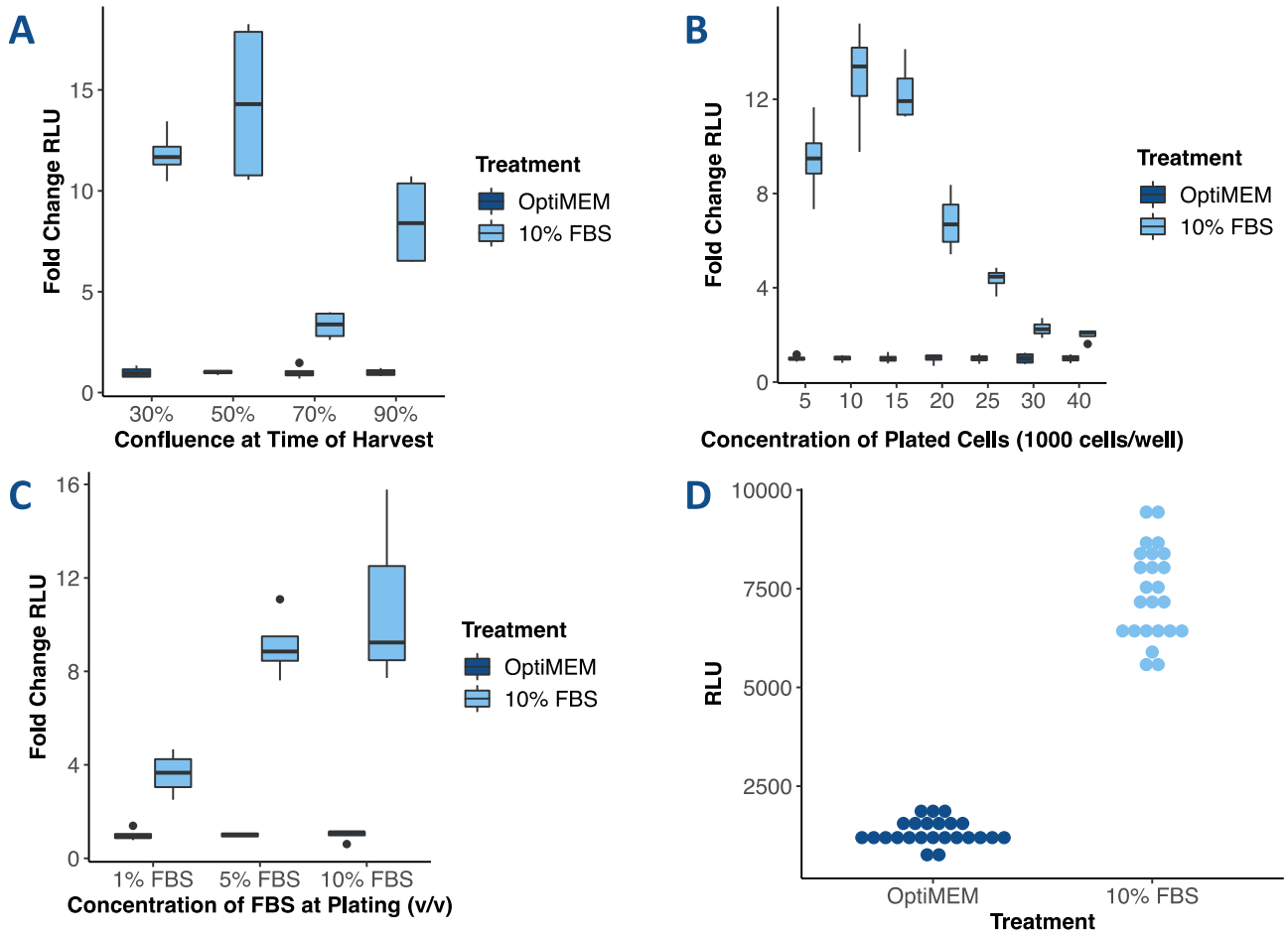

Figure 1: Optimization of Luciferase and β-Galactosidase assays in preparation for the Orphan Receptor Screen. For each receptor HTLA cells were transfected with LPAR1 and treated with OptiMEM (vehicle) or 10% FBS (treatment). Fold change is relative to vehicle treatment and measured in relative luminescence units (RLU), the quotient of luciferase and β-galactosidase assay results. **Panel A:** Fold change in RLU treatment *versus* OptiMEM (vehicle) for HTLA cells harvested for plating at a range of 30% to 90% confluence. **Panel B:** Fold change in RLU treatment *versus* for HTLA cells when cell number was varied at time of plating. **Panel C:** Fold change in RLU *versus* FBS concentration on plated HTLA cells (v/v). **Panel D:** RLU *versus* treatment condition for cells plated with 5% FBS, at 25,000 cells/well and with cell confluence of < 50% at time of harvest.

A 3-(4,5-Dimethylthiazol-2-yl)-2,5-Diphenyltetrazolium Bromide **(**MTT) viability assay was used to determine sweetener toxicity in HTLA cells (Figure 2). Cell viability increased with low concentrations of artificial sweetener for sucralose but not saccharin. Decreases in viability were observed at sweetener concentrations greater than the literature EC50 value for each sweetener acting on T1R2/T1R3. As such, the treatment concentration range used for the orphan receptor screen was selected to capture anticipated potential action of the sweeteners on the orphan receptors while mitigating toxicity to the cells. Chosen treatment concentrations for saccharin and sucralose were 1 mM and 300 µM, respectively (Figure 2).

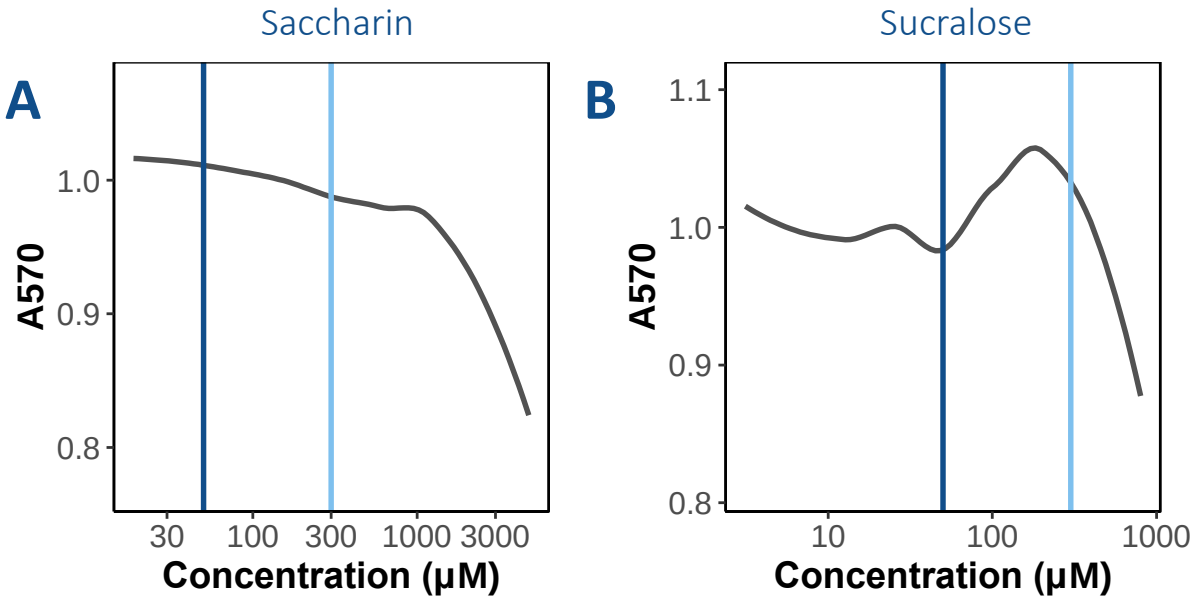

Figure 2: Toxicity of saccharin and sucralose, as measured by 3-(4,5-Dimethylthiazol-2-yl)-2,5-Diphenyltetrazolium Bromide (MTT) assay with absorbance at 570 nm (A570) *versus* Concentration (µM). HTLA cells were treated at 48 hours post plating with serum free media containing saccharin (**Panel A**) or sucralose (**Panel B**) across a range of doses. Cells were incubated for an additional 24 hours before performing an MTT assay. Lines in dark blue show literature EC50 values for activation of T1R2/T1R3 by the respective sweetener while lines in light blue show the treatment concentration used for the screen. The shaded grey area surrounding the smoothed regression indicates CI = 95%.

The orphan receptor screen was conducted with 72 receptors found within the PRESTO-Tango library. LPAR1 activation by 10% FBS, which contains the LPAR1 ligand LPA, was used as a positive control for transfection and cell health on the day of the experiment. Orphan receptors were treated with a combination of sweeteners at the concentrations chosen in Figure 2.

GPR17 and GPR52 activity was significantly increased in response to the sweetener treatment (Table 1; Figure 3A). GPR17 activity was significantly elevated for 2 of 3 biological replicates and when all three replicates were combined. Likewise, not all increases were significant for GPR52, but together the p-value was less than 0.05 (Table 1; Figure 3B). Therefore, GPR17 and GPR52 with associated increases of 1.3-fold and 2.0-fold respectively for treatment with combined sucralose and saccharin relative to control were selected for further investigation and validation of receptor-agonist pairings.

Table 1: Orphan Receptor Screen Statistics; GPCR Receptor numbers and names, fold change, SEM in relative luminescence units (RLU) and p-value of 72 orphan receptor activation in response to treatment with a combination of sucralose and saccharin. For each receptor, HTLA cells were transfected *via* polyethylenimine (PEI) at 24 hours-post-plating. Cells were treated for 24 hours with OptiMEM (vehicle) or a combination of 1 mM saccharin and 300 µM sucralose (treatment). Transfection efficiency and receptor activation were quantified through β-galactosidase and luciferase assays respectively.

Receptor Number	Receptor Name	Fold Change RLU	SEM	p-value	Receptor Number	Receptor Name	Fold Change RLU	SEM	p-value
R01	CMKOR1	1.02	0.07	0.730	R37	GPR32	1.11	0.23	0.387
R02	GPER	0.94	0.10	0.273	R38	GPR35	0.99	0.11	0.586
R03	GPR101	1.24	0.11	0.931	R39	GPR37	0.92	0.11	0.911
R04	GPR110	1.16	0.19	0.655	R40	GPR37L1	1.25	0.20	0.382
R05	GPR113	0.83	0.07	0.072	R41	GPR39	0.86	0.10	0.296
R06	GPR116	1.23	0.16	0.379	R42	GPR4	1.58	0.20	0.211
R07	GPR12	1.36	0.13	0.083	R43	GPR45	0.94	0.12	0.205
R08	GPR123	0.85	0.08	0.846	R44	GPR52	1.85	0.19	0.015
R09	GPR132	0.82	0.08	0.636	R45	GPR55	1.16	0.17	0.546
R10	GPR133	1.50	0.22	0.888	R46	GPR6	1.05	0.18	0.605
R11	GPR141	1.17	0.18	0.383	R47	GPR61	0.80	0.07	0.502
R12	GPR142	1.23	0.18	0.528	R48	GPR62	1.39	0.35	0.596
R13	GPR143	1.46	0.26	0.331	R49	GPR63	0.81	0.11	0.297
R14	GPR144	1.39	0.20	0.980	R50	GPR64	1.08	0.14	0.931
R15	GPR146	1.07	0.15	0.436	R51	GPR78	1.16	0.14	0.912
R16	GPR148	1.31	0.15	0.670	R52	GPR83	1.51	0.45	0.931
R17	GPR149	0.89	0.12	0.224	R53	GPR84	1.10	0.15	1.000
R18	GPR15	0.86	0.11	0.022	R54	GPR85	0.95	0.19	0.863
R19	GPR150	1.01	0.08	0.816	R55	GPR87	0.74	0.11	0.297
R20	GPR151	1.01	0.12	0.891	R56	GPR88	1.90	0.73	0.387
R21	GPR153	0.81	0.14	0.666	R57	GPR54	1.02	0.13	0.634
R22	GPR156	1.09	0.10	0.863	R58	MAS1	1.12	0.11	0.708
R23	GPR160	0.82	0.14	0.546	R59	MAS1L	0.74	0.10	0.052
R24	GPR161	1.10	0.24	0.931	R60	MRGPRD	3.52	2.47	1.000
R25	GPR162	1.01	0.11	0.870	R61	MRGPRF	1.35	0.06	0.452
R26	GPR17	1.29	0.10	0.016	R62	MRGPRG	2.06	1.27	0.222
R27	GPR171	1.26	0.07	0.081	R63	MRGPRX1	1.48	0.30	0.258
R28	GPR173	1.01	0.09	0.563	R64	MRGPRX2	0.75	0.08	0.436
R29	GPR182	0.97	0.08	0.500	R65	MRGPRX4	1.85	0.45	0.277
R30	GPR19	0.79	0.10	0.164	R66	OPN3	0.90	0.13	0.917
R31	GPR20	0.97	0.12	0.312	R67	OPN5	0.81	0.05	0.190
R32	GPR23	0.89	0.10	0.605	R68	PK2	1.13	0.11	0.449
R33	GPR25	0.85	0.08	0.529	R69	PRP	0.95	0.18	0.436
R34	GPR26	1.12	0.10	0.546	R70	TAAR5	1.03	0.18	1.000
R35	GPR27	1.45	0.34	0.815	R71	TAAR6	0.70	0.07	0.077
R36	GPR31	1.21	0.13	0.439	R72	TAAR9	0.75	0.09	0.436

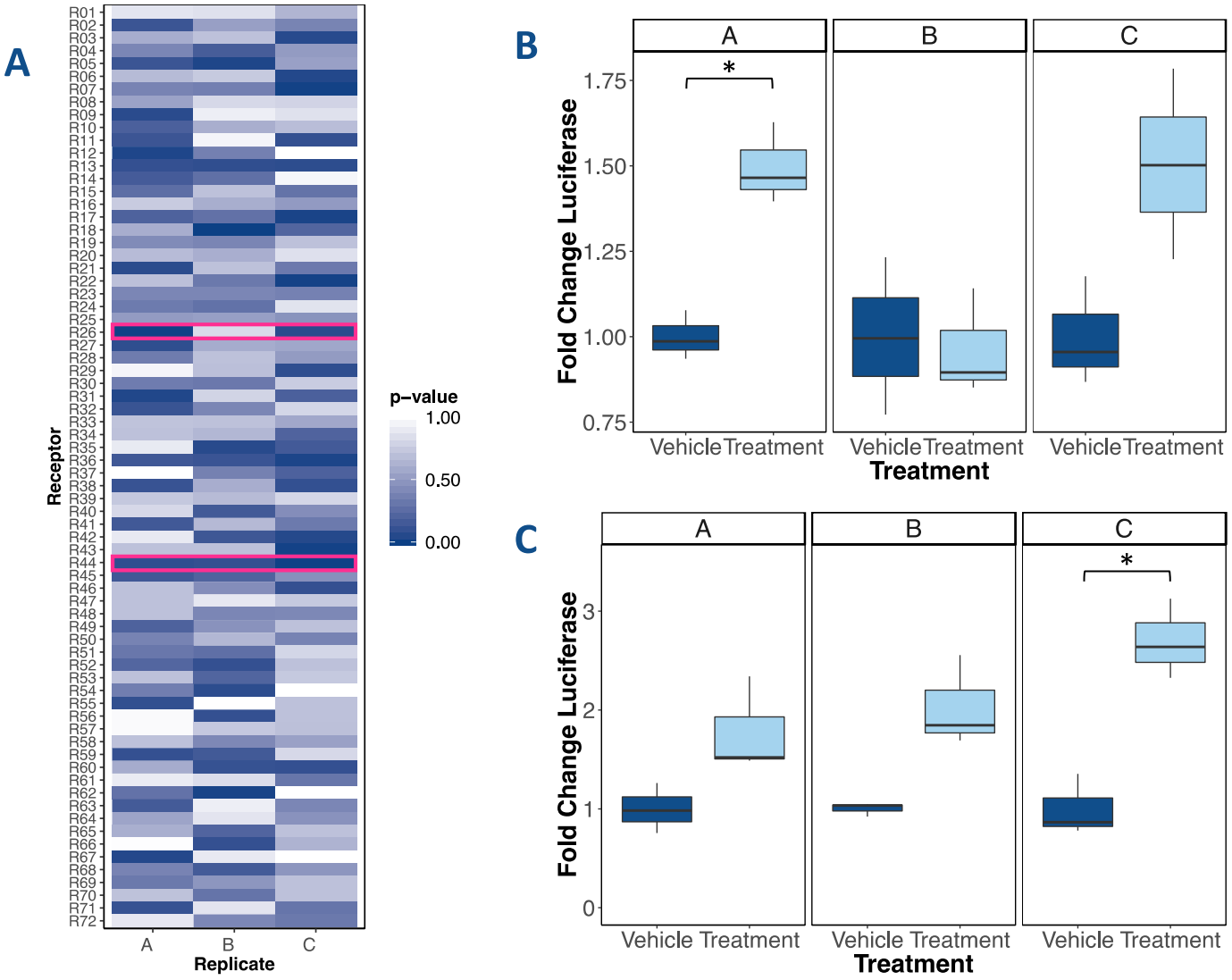

Figure 3: Orphan receptor screen heatmap; **receptor activation in response to combination treatment of the artificial sweeteners, saccharin and sucralose (n=3).** HTLA cells were transfected with one of 72 orphan receptors and treated for 24 hours with OptiMEM (vehicle) or a combination of 1 mM saccharin and 300 µM sucralose (treatment). Transfection efficiency and receptor activation were quantified through β-galactosidase and luciferase assays respectively. The three biological replicates conducted are represented as A, B and C. **Panel A:** Heatmap of all 72 orphan receptors assayed. P-value was determined through statistical comparison by t-test between vehicle and artificial sweetener treatments. GPR17 and GPR52 are indicated by pink boxes surrounding R26 and R44, respectively. **Panels B/C:** HTLA cells were transfected with GPR17-Tango construct **(Panel B)** or GPR52-Tango construct (**Panel C)**. Fold change is measured in luminescence, the output of the luciferase assay and expressed relative to vehicle treatment. For each boxplot, the middle bar represents the median of the data, while the upper and lower hinges show the 3rd and 1st quantiles, respectively. Error bars extend to the highest and lowest points of the dataset. $p < 0.05$ = (*).

While the purpose of the orphan receptor screen presented in Figure 3 was to determine the extent of GPCR activation in response to sucralose and saccharin, the serum-free media control condition provided novel information as well. OptiMEM was used to treat all vehicle conditions in the receptor screen; however, basal luciferase activity greatly differed between cells transfected with different GPCRs as a result of constitutive activity. The Kroeze lab, who developed the orphan GPCR vectors and PRESTO adaptation of the Tango assay, reported a similar experiment to the receptor screen where a panel of GPCRs were treated with standard culture media to quantify their constitutive activity. In the case of our study, however, cells were grown in media containing 10% serum, which contains diverse bioactive components including signaling lipids and growth hormones. Therefore, differences between control data for orphan receptors is likely to be partially caused by the activity of compounds found within FBS.

Comparison of Rourke and Kroeze group reports determined that more than 22% of the 72 receptors were more than twice as active in the Kroeze lab dataset (Figure 4). Both of the receptors which were significantly activated in the orphan receptor screen, GPR17 and GPR52, belonged to this set of constitutively active receptors. GPR17 activity was elevated by 6.2-fold and 18-fold in the Rourke and Kroeze reports respectively, relative to basal activity of LPAR1, the deorphanized receptor used as a positive control in the receptor screen. GPR52 was depressed by 0.47-fold for the Rourke group but elevated by 3.2-fold for the Kroeze group, again relative to LPAR1.

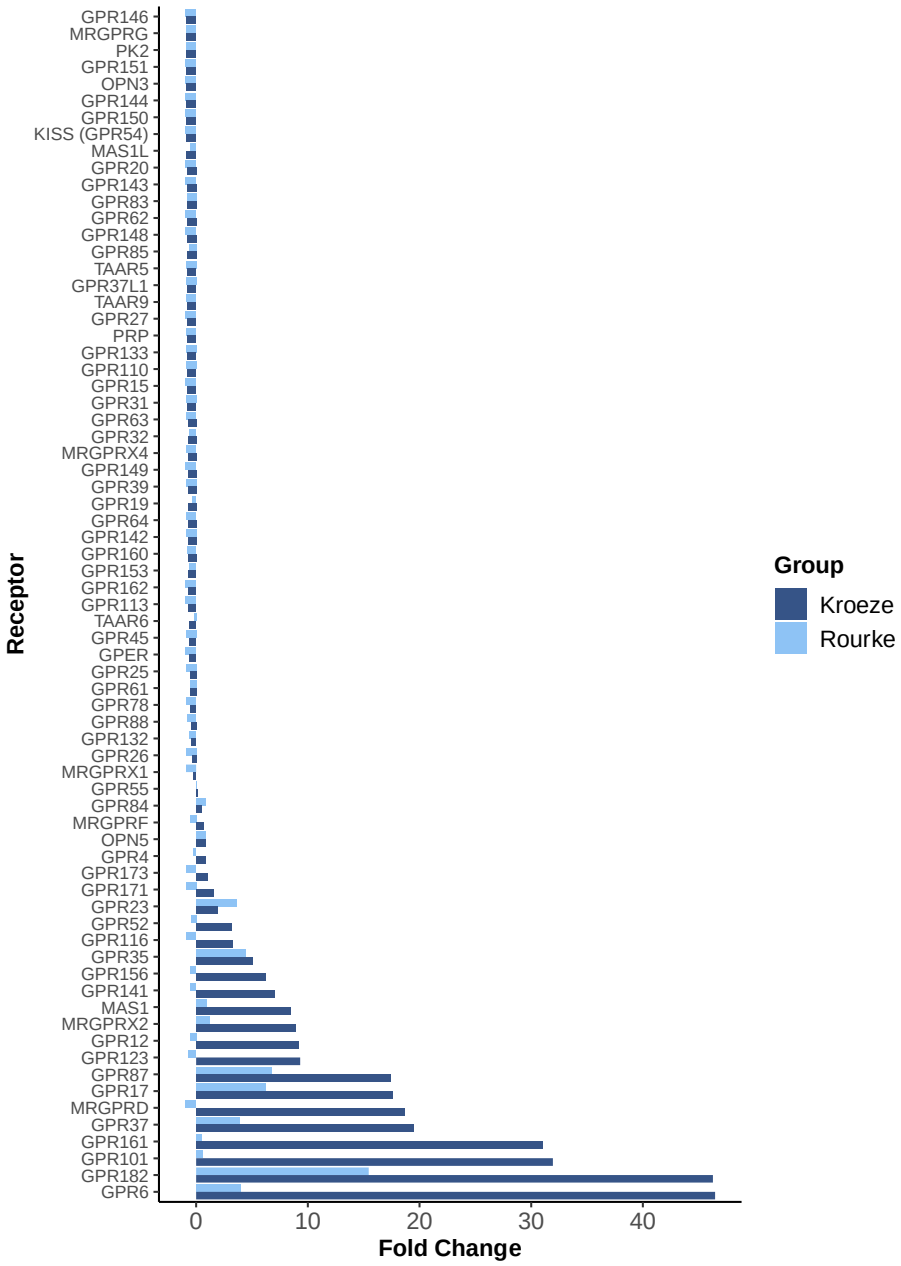

Figure 4: Comparison of constitutive activity measured in fold change luciferase measurement of PRESTO-Tango orphan GPCRs relative to LPAR1 for experimental data (light blue) and data published by Kroeze *et al.* (2014);(dark blue): Data are from the group who developed the PRESTO-Tango platform (Kroeze *et al.,* 2014). **Light blue:** For each receptor, HTLA cells were plated at 25,000 cells/well in high-glucose DMEM with 5% FBS and transfected *via* polyethylenimine (PEI) at 24 hours post plating, before vehicle treatment with serum-free media. Cells were incubated for an additional 24 hours before being lysed and frozen. Cell lysates were thawed and receptor activation was quantified through luciferase assay.

To determine the reproducibility of the significant response observed for the combination of sucralose and saccharin, validation experiments were performed by treating the two activated receptors, GPR17 and GPR52, with sweeteners either individually or in combination. For GPR17, there was an upward trend in cells treated with either sweetener relative to vehicle; however, this difference was not statistically significant for any treatment (Figure 5A). Treatment with saccharin or sucralose led to average increases of 22% ($p = 0.824$) and 55% ($p = 0.196$) respectively, while a combination of the two led to the greatest change with an increase of 61% ($p = 0.114$). Treatment of GPR52 with sucralose differed significantly from both the vehicle and saccharin groups (Figure 5B). Saccharin treatment resulted in an increase of 7.8% while treatment with sucralose led to GPR52 activation increase of over 110% ($p = 0.013$), both relative to control. GPR52 was activated by 85% when treated with a combination of sucralose and saccharin ($p= 0.052$).

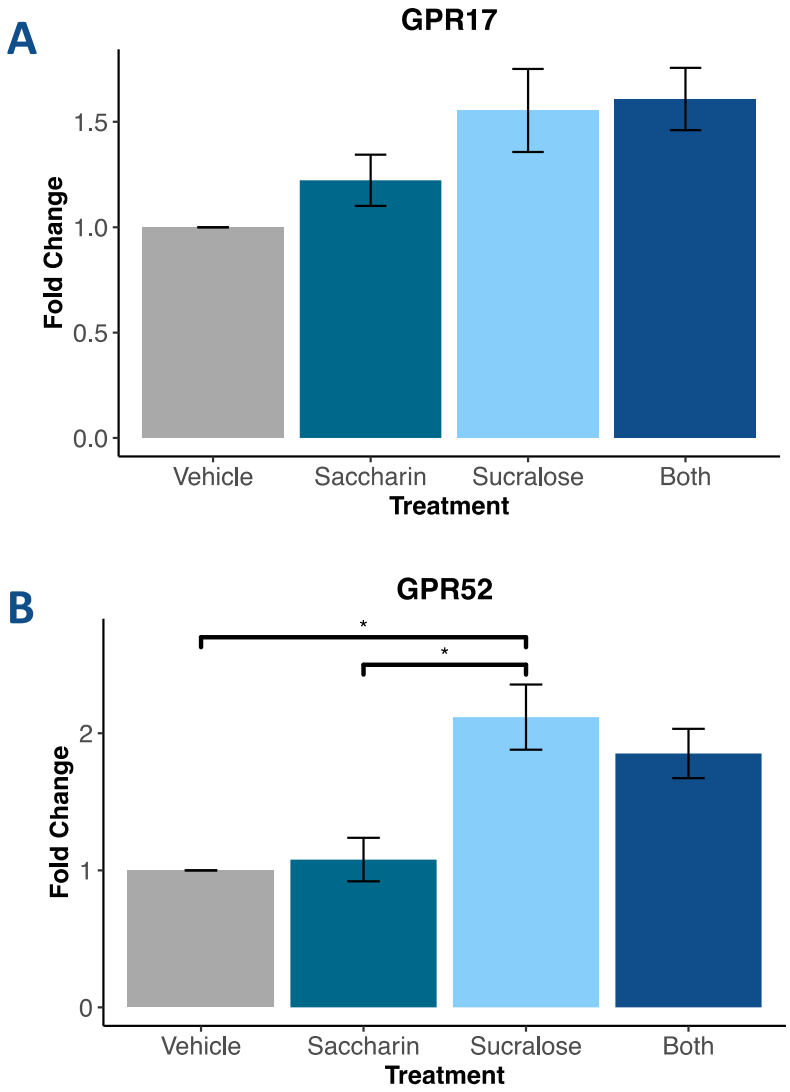

Figure 5: Validation of receptor activation in response to treatment with saccharin and sucralose (n=3). For each receptor, HTLA cells were transfected with GPR17 (**Panel A**) or GPR52 (**Panel B**). Cells were then treated for 24 hours with 1 mM saccharin, 300 µM sucralose or both before lysis. Transfection efficiency and receptor activation were quantified through β-galactosidase and luciferase assays, respectively. Fold change is relative to vehicle treatment and measured in relative luminescence units (RLU), the quotient of luciferase and β-galactosidase assay results. $p < 0.05$ = (*).

To investigate the dose-dependent relationship between the identified GPCRs and sweetener activation, GPR17 and GPR52 were each treated with a wide dose range of each sweetener. GPR17 was activated in response to both artificial sweeteners and the natural sugar sucrose; however, this response demonstrated inhibition by ligand at concentrations above 2 mM (Figure 6A). GPR17 activation was increased to a maximum of 1.5-fold, 1.6-fold and 2.1-fold for 2 mM saccharin, 2 mM sucralose and 2 mM sucrose respectively. GPR52 was activated by the two artificial sweeteners but not sucrose. GPR52 activation was not saturated at any sweetener treatment concentration tested, even above concentrations known to be toxic to human cells (Figure 6B). GPR52 activation reached a maximum value of 5.2-fold for 4 mM sucralose and 5.0-fold for 8 mM saccharin. Sucrose activation of GPR52 was maximally 1 mM with a 1.3-fold increase.

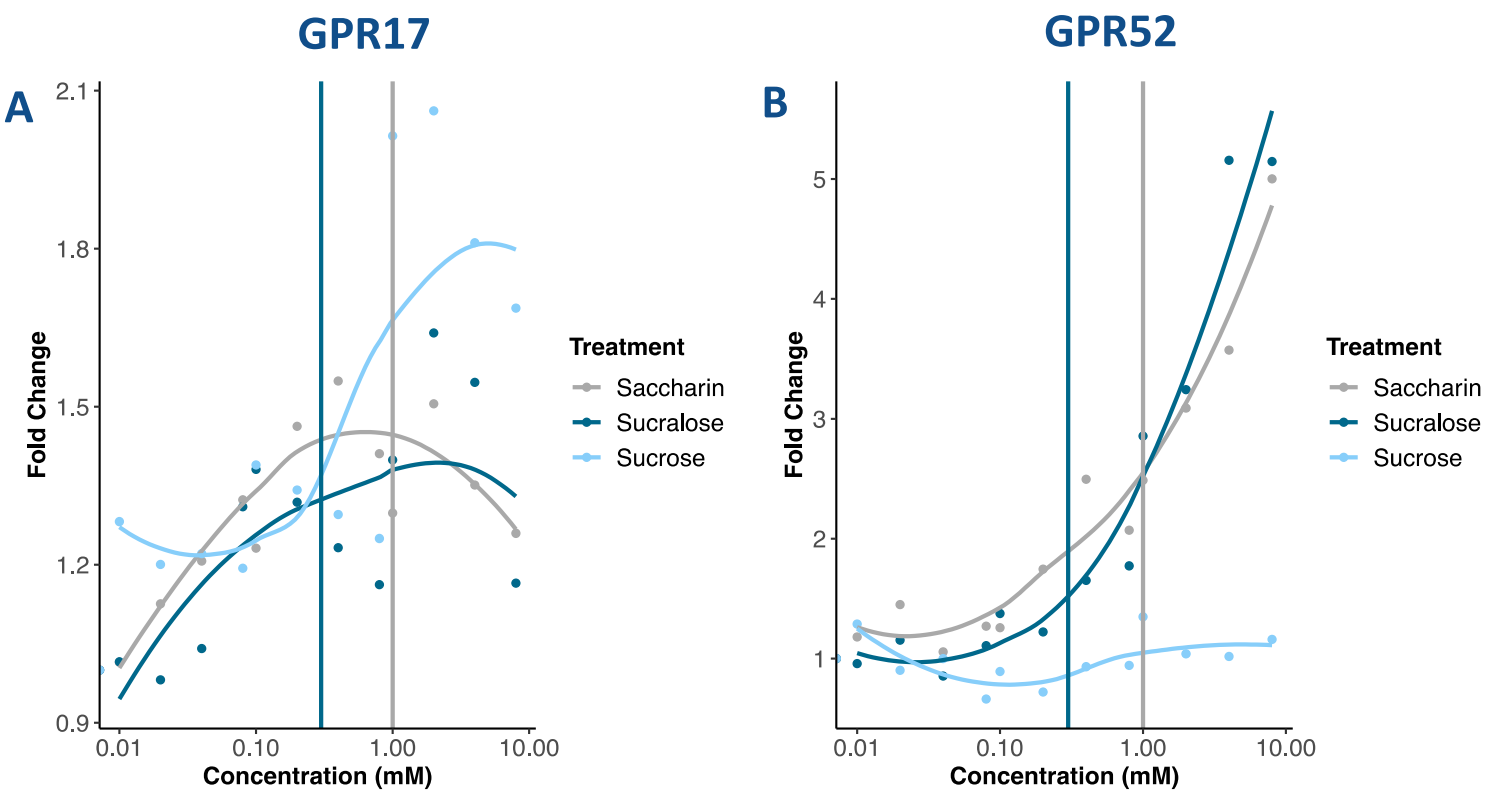

Figure 6: Dose response curves of orphan GPCRS in response to treatment with sucrose, saccharin or sucralose. For each receptor, HTLA cells were transfected with GPR17 (**Panel A**) or GPR52 (**Panel B**). Cells were treated for 24 hours with saccharin, sucralose or sucrose over a range of 0.01 mM to 8 mM. Transfection efficiency and receptor activation were quantified through β-galactosidase and luciferase assays, respectively. Fold change is measured in relative luminescence units, the quotient of luciferase and β-galactosidase assay results and expressed relative to vehicle control treatment (not shown). Dark blue and grey lines represent EC50 values for sucralose and saccharin activation of T1R2/T1R3, respectively.

Discussion

This study aimed to better characterize the molecular effects of artificial sweeteners on the human body by screening 72 orphan receptors with sucralose and saccharin. GPR17 and GPR52 were the only two orphan receptors which were significantly activated in response to combined sucralose and saccharin (Table 1). Validation of receptor activity confirmed that GPR17 and GPR52 were activated by the cocktail of artificial sweeteners, but that sucralose was responsible for the majority of the effect observed in the screen (Figure 5). Dose response curves established that saccharin and sucralose activate both receptors, but that GPR52 is activated to a greater extent than GPR17 (Figure 6).

Constituitive Activity

Differences in orphan receptor activity between this report and the Kroeze group experiment point to ligand receptor pairings beyond artificial sweeteners (Figure 4). Our findings suggest that compounds found within FBS cause activation of 16 of the orphan receptors which were twice as active in the Kroeze group report. FBS, a complex mixture of lipids, proteins and saccharides, presents a greatly reduced library of compounds compared with the tens of thousands of metabolites found within the human body.

To confirm that FBS is responsible for activating these receptors, the receptor screen experiment could be replicated with treatment of several dosage levels of FBS. Receptors which follow a dose dependent increase in activation could then be investigated further by isolating compounds found within FBS to identify individual ligands. Constitutively active receptors present promising targets for drug discovery for several reasons. High baseline activity leads to large signal to noise ratios, allowing the use of a greater number of high-throughput techniques while keeping false positives and negatives at a minimum (Zhang et al., 2016). This subset of receptors is also of interest to medicinal chemists who are now developing drugs which aim to regulate GPCR signalling through allosteric action instead of orthosteric activation or inhibition (Conn et al., 2009). Compounds which act allosterically instead of at the orthosteric site

produce fewer off-target effects because they can only modify the signal when the endogenous ligand is present and the GPCR is already signalling.

Receptor Validation and Dose Response

Initial hits from the high-throughput orphan receptor screen were confirmed through triplicate validation experiments of sweeteners alone or in combination. In contrast to the receptor screen, differences between vehicle and combination treatments were found to be non-significant likely because of the reduced statistical power used in the second analysis. However, validation experiments revealed that the majority of the increase in receptor activation was caused by sucralose, not saccharin (Figure 5).

Dose response curves were conducted with a panel of artificial and natural sweeteners. The magnitude of receptor activation in response to either sweetener was greater for GPR52 relative to GPR17 (Figure 6A; 6B). While GPR17 was activated by more then 2-fold by sucrose, GPR52 was not measurably activated. This points to interactions with functional groups like benzene rings and chloride within the active site, which are found on the artificial sweeteners tested but not sucrose. Furthermore, this also provides evidence supporting a more ideal site for allosteric modulation in drug development as the receptor will face less interference from ubiquitous endogenous compounds. Estimated EC50 values from these dose response curves remain well below that of known potency of artificial sweeteners on T1R2/T1R3; however, greater assay sensitivity is required to definitively quantify EC50 values and how they may differ from that of known sweet-sensing receptors. Glucose, aspartame and acesulfame K were also assayed through dose response curves with GPR17 and GPR52, however low signal and high variability prohibited definitive conclusions (data not shown). Greater assay sensitivity is required to definitively explain the relationship between the sweeteners and receptors.

GPR17

Molecular dynamics studies have shown that the binding pocket of GPR17 contains several key binding residues for functional groups found on saccharin,

sucralose and sucrose. (Saravanan et al., 2018). Synthetic compounds that activate GPR17 contain both monocyclic and heterocyclic structures which readily bind Phe_{111}. Chlorinated rings, like those in sucralose have multiple binding partners including Tyr_{112}, His_{252} and Val_{253}. Together, these findings suggest that saccharin and sucralose share structural similarity with synthetic compounds known to bind GPR17. A relatively large amount is known about GPR17, despite being an orphan receptor. GPR17 is a constitutively active receptor, meaning that it is capable of signalling through G_i to inhibiting the production of cAMP even without the presence of a known ligand (Fumagalli et al., 2016). It is expressed throughout the central nervous system (CNS) and particularly in tissues which are commonly subject to ischemic damage. Up to this point, targeted investigation of GPR17 has focused on the nature of the receptor in relation to structurally homologous de-orphanized receptors like P2Y, a family of receptors which participates in purinergic signalling (Fumagalli et al., 2016). Additionally, two isoforms of GPR17 have been discovered in the human genome, the first of 339-amino acids and a second with an additional 28-amino acid extension in the extracellular domain, the latter of which was tested in this study (Marucci et al., 2019). GPR17 localization within the CNS has been linked to its role in driving the maturation of oligodendrocytes, the glial-like cells responsible for the myelination of neurons. High GPR17 expression prevents activation of adenylyl cyclase (AC), as a low level of cAMP is necessary for maturation of this cell type. Only when the cells approach maturity is GPR17 downregulated and internalized, allowing intracellular concentrations of cAMP to normalize (Fumagalli et al., 2016). Additionally, GPR17 is induced in response to acute trauma in damaged neurons where it has been associated with increasing myelin repair and driving maturation and propagation of surrounding oligodendrocytes (Fumagalli et al., 2016). As such, the receptor likely plays a large role in recovery from ischemic trauma in organs such as the heart, brain and spinal cord.

Furthermore, recent work suggests that drugs which are able to control the activation of GPR17 may have direct application in the pathogenesis of neurodegenerative conditions which are partially or fully caused by demyelination, including multiple sclerosis, Alzheimer's disease and ischemic stroke (Marucci et al., 2019). Greater investigation of compounds which activate this receptor promise to

provide better understanding of the mechanism of healing previously difficult cases with ischemic damage. In this way, further investigation of cellular response to GPR17 activation through sweeteners, particularly as it relates to CNS function and neuronal signalling is important to future work conducted on this relationship.

While GPR17 has been the subject of a variety of studies to fully determine possible agonists, suggested activation by the immunomodulators LTC4, LTD4 and uracil has been called into question based on the lack of biological activity in cell models expressing this receptor (Kanaoka and Boyce, 2014). This highlights the challenge in continuing forward with investigating artificial sweetener activation of GPR17 or GPR52; the ligand-receptor pairing must induce a measurable biological change to confirm that the effect is relevant. Future studies should begin by investigating the Gα signalling pathways associated with each receptor to ensure that they are above the threshold to induce significant changes in intracellular signalling.

GPR52

GPR52 is another GPCR which is expressed throughout the CNS and most specifically in the brain; however, few studies describe GPR52 deorphanization or characterization. GPR52 has been found to be colocalized with the G_s-coupled D1 dopamine receptor and G_i-coupled D2 dopamine receptor in the cortex and striatum, respectively. GPR52 is coupled to the cAMP generating G_s pathway which is associated with pro-cognitive and antipsychotic effects (von Heimendahl et al., 2016). *In vitro* experiments of rat brain slices have shown that GPR52 can be activated by tool compounds and causes a sustained increase of post synaptic excitatory signalling, which is associated with pro-cognitive effects (von Heimendahl et al., 2016). Rat knockouts show that loss of GPR52 causes psychotic phenotype while those with transgenically upregulated GPR52 demonstrate that gain of promotes antipsychotic behaviours (Komatsu et al., 2014). Recent work has established that reserpine, an antipsychotic drug used for the treatment of schizophrenia, is able to activate GPR52 through the Gs pathway and induce Ca^{2+} signalling. However, an endogenous ligand for GPR52 has yet to be established (Komatsu et al., 2014). Better understanding of the function of GPR52 associated with improving psychotic and neurodegenerative

pathology is critical to the potential of any new ligands or drugs associated with this receptor.

Recently crystal structures of GPR52 suggest that like GPR17, this receptor is constitutively active (Lin et al., 2020). Extracellular loop 2 (ECL2), a short linker sequence which joins two transmembrane alpha helices, fills the orthosteric pocket in this receptor and causes constant receptor activation while blocking other molecules from entering. This suggests that sucralose and saccharin must bind at a small side pocket in the N-terminal of GPR52, interacting with residues His_{25}, Ser_{26}, Ile_{89} and Phe_{117}. Crystal structures of GPR52 with the putative allosteric agonist c17 indicate that small molecule binding is able to modify the structure of GPR52 without altering receptor-ECL2 binding. This provides a mechanism for artificial sweetener activation of GPR52, where allosteric binding is able to upregulate constitutive signalling.

It should be noted, however, that current annotation of healthy human samples does not show elevated levels of GPR17 or GPR52 expression in tissues other than those found within the CNS, including absences within adipose tissue, epithelium and the pancreas (Uhlén et al., 2015). However, this does not preclude sensing of sweet molecules by induction in disease states, but as of now there exists no evidence to support this theory.

The CNS has also been directly implicated in the control of glucose metabolism and GPR17 and GPR52 may be involved in this process. The arcuate nucleus of the hypothalamus is the most widely studied neurocircuitry which regulates glucose homeostasis (Arble and Sandoval, 2013). This neuron cluster is responsive to both insulin and nutrients like glucose and fatty acids which activate K_{ATP} channels and lead to signalling which suppresses hepatic glucose production (Arble and Sandoval, 2013). This demonstrates the direct and systemic role that the CNS has in glucose metabolism. Psychotic disorders linked to GPR52 have been linked to disruption of glucose metabolism as well. Meta-analysis of patients with schizophrenia show that they are 3 times more likely to develop metabolic diseases like type 2 diabetes (Mitchell et al., 2013). Much of this effect has been attributed to the inflammation surrounding this condition, but it is possible that GPR52 contributes to this comorbidity. Currently, no databases exist which compare genomic expression of GPCRs between neurotypical

and schizophrenic patients, but once available, this information could establish a role for GPR52 in this relationship.

Strengths and Limitations

MTT Assay

The MTT assay has been considered the gold standard of cytotoxicity assay since its inception as the first non-radioisotopic measure of cell viability. The generation of insoluble formazan crystals from MTT through the redox activity of cellular respiration produces a stable static endpoint for the assay which can be easily and accurately measured with a microplate spectrophotometer. However, a recent report suggests that the MTT assay is less accurate and less sensitive to changes in cell populations in comparison to newer enumeration assays including sulforhodamine B and neutral red uptake (van Tonder et al., 2015).

PRESTO Tango Assay

The PRESTO Tango system is highly effective for ligand and drug screens with a large number GPCRs. However, this comes at the cost of providing more specific information about the nature of receptor activation and accurate results for receptors with specialized structure or function. This is partially the motivation behind the study design which only included 72 family A GPCRs out of the 90 orphan receptors, as the family B and C receptors have not been successfully validated in the PRESTO Tango platform.

PRESTO-Tango is not the only system in use for high throughput deorphanization of GPCRs. Functional assays which measure native downstream effects of GPCR activation are also used; however, they require specific cellular responses to be initiated by the receptor for detection. Assays which quantify calcium or cAMP concentration in the cytoplasm fall into this category and can inform the effect that the orphan receptor might have, but Gα proteins are not always known for orphan GPCRs (Tunaru, 2017).

Given the variable nature of the PRESTO Tango assay, three replicates were completed for all receptors in the orphan receptor screen. Increases were not significant

for all replicates of GPR17 or GPR52, however low variability across replicates demonstrates high quality data from the screen. In this case, higher statistical power coming from the greater number of replicates conducted for each condition allowed statistical significance to carry through, even in cases with greater variability.

Dose response curve findings remain preliminary as only one biological replicate of this experiment could be conducted to date due to difficulties in replicating and isolating plasmid DNA for the two receptor vectors. More work must be completed in chemically competent *E. coli* to general a reliable source of plasmid DNA.

Conclusion & Future Directions

Through the first interrogation of Rhodopsin class (Family A) orphan GPCRs with sucralose and saccharin, two novel receptor-agonist pairings for GPR17 and GPR52 were discovered and characterized. The ability of these sweeteners to activate both receptors and potentially increase neuro-protective signalling functions is a promising start which may eventually lead to drug development of sweetener analogues that allosterically activate these receptors. Due to the many ways in which artificial sweeteners interact with GPCRs throughout the body, this report promises to better develop the picture of how the body responds to both natural and artificial sweeteners.

This study does not completely characterize the ligand-receptor relationship between GPR17, GPR52 and artificial sweeteners. Dose response curves, like those reported here, must be conducted with higher numbers of biological replicates to confirm responses, higher concentrations of sweeteners and with higher sensitivity luciferase assay reagents to more accurately determine pharmacological parameters such as EC50. These relationships require confirmation of physiological and signalling responses in cells which naturally express the GPR17 or GPR52, beginning by confirming which Gα proteins are activated in response to sucralose or saccharin.

GPR17 and GPR52 represent putative sweet-sensing receptors and an advanced understanding of their signaling and physiological function promise to contribute to a more complete understanding of sweet molecule sensing and metabolic disease in relation to artificial sweetener consumption.

References

Abou-Donia, M.B., El-Masry, E.M., Abdel-Rahman, A.A., McLendon, R.E., and Schiffman, S.S. (2008). Splenda alters gut microflora and increases intestinal p-glycoprotein and cytochrome p-450 in male rats. J Toxicol Environ Health Part A *71*, 1415–1429.

Arble, D.M., and Sandoval, D.A. (2013). CNS Control of Glucose Metabolism: Response to Environmental Challenges. Front Neurosci *7*.

Barnea, G., Strapps, W., Herrada, G., Berman, Y., Ong, J., Kloss, B., Axel, R., and Lee, K.J. (2008). The genetic design of signaling cascades to record receptor activation. PNAS *105*, 64–69.

Chattopadhyay, S., Raychaudhuri, U., and Chakraborty, R. (2014). Artificial sweeteners – a review. J Food Sci Technol *51*, 611–621.

Civelli, O. (2012). Orphan GPCRs and neuromodulation. Neuron *76*, 12–21.

Conn, P.J., Christopoulos, A., and Lindsley, C.W. (2009). Allosteric modulators of GPCRs: a novel approach for the treatment of CNS disorders. Nat Rev Drug Discov *8*, 41–54.

Depoortere, I. (2014). Taste receptors of the gut: emerging roles in health and disease. Gut *63*, 179–190.

Díez-Sampedro, A., Hirayama, B.A., Osswald, C., Gorboulev, V., Baumgarten, K., Volk, C., Wright, E.M., and Koepsell, H. (2003). A glucose sensor hiding in a family of transporters. PNAS *100*, 11753–11758.

van Eyk, A.D. (2015). The effect of five artificial sweeteners on Caco-2, HT-29 and HEK-293 cells. Drug Chem Toxicol *38*, 318–327.

Fang, Y., Kenakin, T., and Liu, C. (2015). Editorial: Orphan GPCRs As Emerging Drug Targets. Front Pharmacol *6*, 295.

Fournel, A., Marlin, A., Abot, A., Pasquio, C., Cirillo, C., Cani, P.D., and Knauf, C. (2016). Glucosensing in the gastrointestinal tract: Impact on glucose metabolism. Am J Physiol Gastrointest Liver Physiol *310*, G645–G658.

Fumagalli, M., Lecca, D., and Abbracchio, M.P. (2016). CNS remyelination as a novel reparative approach to neurodegenerative diseases: The roles of purinergic signaling and the P2Y-like receptor GPR17. Neuropharmacology *104*, 82–93.

Geraedts, M.C.P., Troost, F.J., and Saris, W.H.M. (2011). Different tastants and low-caloric sweeteners induce differential effects on the release of satiety hormones. Food Chem *129*, 731–738.

Gurevich, V.V., and Gurevich, E.V. (2019). GPCR Signaling Regulation: The Role of GRKs and Arrestins. Front Pharmacol *10,* 125.

Harmar, A.J. (2001). Family-B G-protein-coupled receptors. Genome Biol *2*, 3013.1-10.

Harpaz, D., Yeo, L.P., Cecchini, F., Koon, T.H.P., Kushmaro, A., Tok, A.I.Y., Marks, R.S., and Eltzov, E. (2018). Measuring Artificial Sweeteners Toxicity Using a Bioluminescent Bacterial Panel. Molecules *23*, E2454.

Hauser, A.S., Attwood, M.M., Rask-Andersen, M., Schiöth, H.B., and Gloriam, D.E. (2017). Trends in GPCR drug discovery: new agents, targets and indications. Nat Rev Drug Discov *16*, 829–842.

von Heimendahl, M., Arban, R., Deiana, S., Hobson, S., Rosenbrock, H., and Schülert, N. (2016). PM537. GPR52 agonists show pro-cognitive properties. Int J Neuropsychopharmacol *19*, 95–95.

Holst, J.J. (2007). The physiology of glucagon-like peptide 1. Physiol Rev *87*, 1409–1439.

Hu, G.-M., Mai, T.-L., and Chen, C.-M. (2017). Visualizing the GPCR Network: Classification and Evolution. Sci Rep *7*, 1–15.

Husted, A.S., Trauelsen, M., Rudenko, O., Hjorth, S.A., and Schwartz, T.W. (2017). GPCR-Mediated Signaling of Metabolites. Cell Metab *25*, 777–796.

Jassal, B., Jupe, S., Caudy, M., Birney, E., Stein, L., Hermjakob, H., and D'Eustachio, P. (2010). The systematic annotation of the three main GPCR families in Reactome. Database (Oxford) *2010*.

Kanaoka, Y., and Boyce, J.A. (2014). Cysteinyl Leukotrienes and Their Receptors; Emerging Concepts. Allergy Asthma Immunol Res *6*, 288–295.

Knauf, C., Cani, P.D., Kim, D.-H., Iglesias, M.A., Chabo, C., Waget, A., Colom, A., Rastrelli, S., Delzenne, N.M., Drucker, D.J., Seeley, R.J., and Burcelin, R. (2008). Role of central nervous system glucagon-like Peptide-1 receptors in enteric glucose sensing. Diabetes *57*, 2603–2612.

Kobilka, B.K. (2007). G Protein Coupled Receptor Structure and Activation. Biochim Biophys Acta *1768*, 794–807.

Komatsu, H., Maruyama, M., Yao, S., Shinohara, T., Sakuma, K., Imaichi, S., Chikatsu, T., Kuniyeda, K., Siu, F.K., Peng, L.S., et al. (2014). Anatomical Transcriptome of G Protein-Coupled Receptors Leads to the Identification of a Novel Therapeutic Candidate GPR52 for Psychiatric Disorders. PLoS One *9*.

Kroeze, W.K., Sassano, M.F., Huang, X.-P., Lansu, K., McCorvy, J.D., Giguère, P.M., Sciaky, N., and Roth, B.L. (2015). PRESTO-Tango as an open-source resource for interrogation of the druggable human GPCRome. Nat Struct Mol Biol *22*, 362–369.

Laffitte, A., Neiers, F., and Briand, L. (2014). Functional roles of the sweet taste receptor in oral and extraoral tissues. Curr Opin Clin Nutr Metab Care *17*, 379–385.

Latek, D., Modzelewska, A., Trzaskowski, B., Palczewski, K., and Filipek, S. (2012). G protein-coupled receptors — recent advances. Acta Biochim Pol *59*, 515–529.

Lee, A.A., and Owyang, C. (2017). Sugars, Sweet Taste Receptors, and Brain Responses. Nutrients *9*, E653.

Leloup, C., Allard, C., Carneiro, L., Fioramonti, X., Collins, S., and Pénicaud, L. (2016). Glucose and hypothalamic astrocytes: More than a fueling role? Neuroscience *323*, 110–120.

Lin, X., Li, M., Wang, N., Wu, Y., Luo, Z., Guo, S., Han, G.-W., Li, S., Yue, Y., Wei, X., et al. (2020). Structural basis of ligand recognition and self-activation of orphan GPR52. Nature *579*, 152–157.

Lv, X., Liu, J., Shi, Q., Tan, Q., Wu, D., Skinner, J.J., Walker, A.L., Zhao, L., Gu, X., Chen, N., et al. (2016). In vitro expression and analysis of the 826 human G protein-coupled receptors. Protein Cell *7*, 325–337.

MacDonald, P.E., El-kholy, W., Riedel, M.J., Salapatek, A.M.F., Light, P.E., and Wheeler, M.B. (2002). The Multiple Actions of GLP-1 on the Process of Glucose-Stimulated Insulin Secretion. Diabetes *51*, S434–S442.

MacDonald, P.E., Joseph, J.W., and Rorsman, P. (2005). Glucose-sensing mechanisms in pancreatic beta-cells. Philos Trans R Soc Lond, B, Biol Sci *360*, 2211–2225.

Magnuson, B.A., Carakostas, M.C., Moore, N.H., Poulos, S.P., and Renwick, A.G. (2016). Biological fate of low-calorie sweeteners. Nutr Rev *74*, 670–689.

Martin, B., Dotson, C.D., Shin, Y.-K., Ji, S., Drucker, D.J., Maudsley, S., and Munger, S.D. (2009). Modulation of taste sensitivity by GLP-1 signaling in taste buds. Ann N Y Acad Sci *1170*, 98–101.

Marucci, G., Ben, D.D., Lambertucci, C., Navia, A.M., Spinaci, A., Volpini, R., and Buccioni, M. (2019). GPR17 receptor modulators and their therapeutic implications: review of recent patents. Expert Opin Ther Pat *29*, 85–95.

McCudden, C.R., Hains, M.D., Kimple, R.J., Siderovski, D.P., and Willard, F.S. (2005). G-protein signaling: back to the future. CMLS, Cell Mol Life Sci *62*, 551–577.

de Mendoza, A., Sebé-Pedrós, A., and Ruiz-Trillo, I. (2014). The Evolution of the GPCR Signaling System in Eukaryotes: Modularity, Conservation, and the Transition to Metazoan Multicellularity. Genome Biol Evol *6*, 606–619.

Merigo, F., Benati, D., Cristofoletti, M., Osculati, F., and Sbarbati, A. (2011). Glucose transporters are expressed in taste receptor cells. J. Anat. *219*, 243–252.

Mitchell, A.J., Vancampfort, D., Sweers, K., van Winkel, R., Yu, W., and De Hert, M. (2013). Prevalence of Metabolic Syndrome and Metabolic Abnormalities in Schizophrenia and Related Disorders—A Systematic Review and Meta-Analysis. Schizophr Bull *39*, 306–318.

Morri, M., Sanchez-Romero, I., Tichy, A.-M., Kainrath, S., Gerrard, E.J., Hirschfeld, P.P., Schwarz, J., and Janovjak, H. (2018). Optical functionalization of human Class A orphan G-protein-coupled receptors. Nat Commun *9*, 1950.

Renwick, A.G. (1985). The disposition of saccharin in animals and man--a review. Food Chem Toxicol *23*, 429–435.

Rosenbaum, D.M., Rasmussen, S.G.F., and Kobilka, B.K. (2009). The structure and function of G-protein-coupled receptors. Nature *459*, 356–363.

Saltiel, A.R., and Kahn, C.R. (2001). Insulin signalling and the regulation of glucose and lipid metabolism. Nature *414*, 799–806.

Sanematsu, K., Yoshida, R., Shigemura, N., and Ninomiya, Y. (2014a). Structure, function, and signaling of taste g-protein-coupled receptors. Curr Pharm Biotechnol *15*, 951–961.

Sanematsu, K., Kusakabe, Y., Shigemura, N., Hirokawa, T., Nakamura, S., Imoto, T., and Ninomiya, Y. (2014b). Molecular Mechanisms for Sweet-suppressing Effect of Gymnemic Acids. J Biol Chem *289*, 25711–25720.

Saravanan, K.M., Palanivel, S., Yli-Harja, O., and Kandhavelu, M. (2018). Identification of novel GPR17-agonists by structural bioinformatics and signaling activation. Int J Biol Macromol *106*, 901–907.

Schuit, F.C., Huypens, P., Heimberg, H., and Pipeleers, D.G. (2001). Glucose sensing in pancreatic beta-cells: a model for the study of other glucose-regulated cells in gut, pancreas, and hypothalamus. Diabetes *50*, 1–11.

Shimizu, M., Goto, M., Kawai, T., Yamashita, A., and Kusakabe, Y. (2014). Distinct Human and Mouse Membrane Trafficking Systems for Sweet Taste Receptors T1r2 and T1r3. PLoS One *9,* e100425.

Shioda, S., Takenoya, F., Yagi, M., Wang, L., Hori, Y., and Kageyama, H. (2008). Neural networks of several novel neuropeptides involved in feeding regulation. Nutrition *24*, 848–853.

Simon, B.R., Parlee, S.D., Learman, B.S., Mori, H., Scheller, E.L., Cawthorn, W.P., Ning, X., Gallagher, K., Tyrberg, B., Assadi-Porter, F.M., et al. (2013). Artificial Sweeteners Stimulate Adipogenesis and Suppress Lipolysis Independently of Sweet Taste Receptors. J Biol Chem *288*, 32475–32489.

Smrcka, A.V. (2008). G protein βγ subunits: Central mediators of G protein-coupled receptor signaling. Cell Mol Life Sci *65*, 2191–2214.

Suez, J., Korem, T., Zeevi, D., Zilberman-Schapira, G., Thaiss, C.A., Maza, O., Israeli, D., Zmora, N., Gilad, S., Weinberger, A., et al. (2014). Artificial sweeteners induce glucose intolerance by altering the gut microbiota. Nature *514*, 181–186.

Sweatman, T.W., Renwick, A.G., and Burgess, C.D. (1981). The pharmacokinetics of saccharin in man. Xenobiotica *11*, 531–540.

Tao, Y.-X. (2008). Constitutive Activation of G Protein-Coupled Receptors and Diseases: Insights into Mechanisms of Activation and Therapeutics. Pharmacol Ther *120*, 129–148.

van Tonder, A., Joubert, A.M., and Cromarty, A.D. (2015). Limitations of the 3-(4,5-dimethylthiazol-2-yl)-2,5-diphenyl-2H-tetrazolium bromide (MTT) assay when compared to three commonly used cell enumeration assays. BMC Res Notes *8*.

Tunaru, S. (2017). Strategies for G-protein coupled receptor deorphanization. Mol Life *1*, 71–79.

Uhlén, M., Fagerberg, L., Hallström, B.M., Lindskog, C., Oksvold, P., Mardinoglu, A., Sivertsson, Å., Kampf, C., Sjöstedt, E., Asplund, A., et al. (2015). Proteomics. Tissue-based map of the human proteome. Science *347*, 1260419.

Wickham, H. (2009). ggplot2: Elegant Graphics for Data Analysis (Springer Publishing Company, Incorporated).

Wright, E.M., Martín, M.G., and Turk, E. (2003). Intestinal absorption in health and disease--sugars. Best Pract Res Clin Gastroenterol *17*, 943–956.

Zhang, F., Klebansky, B., Fine, R.M., Liu, H., Xu, H., Servant, G., Zoller, M., Tachdjian, C., and Li, X. (2010). Molecular mechanism of the sweet taste enhancers. Proc Natl Acad Sci U S A *107*, 4752–4757.

Zhang, J.-H., Chung, T.D.Y., and Oldenburg, K.R. (2016). A Simple Statistical Parameter for Use in Evaluation and Validation of High Throughput Screening Assays. J Biomol Screen *4,* 67-73.

Appendix

A.1 R Code

A.1.1 Code to complete statistical analysis of HTS data

```
library(tidyverse)
library(broom)

df <- read.csv(file.choose(), header=TRUE); df

# Conduct Shapiro tests for normality on each set of receptor triplicates

df.shapiro <- df %>%
  group_by(Receptor, Treatment) %>%
  nest() %>%
  mutate(Shapiro = map(data, ~ shapiro.test(.x$Luc)))

df.shapiro.glance <- df.shapiro %>%
  mutate(glance_shapiro = Shapiro %>% map(glance)) %>%
  unnest(glance_shapiro); df.shapiro.glance

# Conduct Barlett's tests for homogeneity of variences on each set of receptor triplicates

df.bartlett <- df %>%
  group_by(Receptor) %>%
  nest() %>%
  mutate(Bartlett = map(data, ~ bartlett.test(.x$Luc~.x$Treatment)))

df.bartlett.glance <- df.bartlett %>%
  mutate(glance_bartlett = Bartlett %>% map(glance)) %>%
  unnest(glance_bartlett); df.bartlett.glance

# Conduct t-tests (parametric) for statistical on each set of receptor triplicates between
vehicle and treatment

df.ttest <- df %>%
  group_by(Receptor) %>%
  nest() %>%
  mutate(ttest = map(data, ~ t.test(.x$Luc~.x$Treatment)))

df.ttest.glance <- df.ttest %>%
  mutate(glance_ttest = ttest %>% map(glance)) %>%
  unnest(glance_ttest); df.ttest.glance
```

```
# Conduct Wilcox tests (non-parametric) for statistical on each set of receptor triplicates
between vehicle and treatment

df.wilcox <- df %>%
  group_by(Receptor) %>%
  nest() %>%
  mutate(wilcox = map(data, ~ wilcox.test(.x$Luc~.x$Treatment)))

df.wilcoxtest.glance <- df.wilcox %>%
  mutate(glance_wilcox = wilcox %>% map(glance)) %>%
  unnest(glance_wilcox); df.wilcoxtest.glance

# Combine p-values into a single table and output

shapiro.p <-
  df.shapiro.glance %>%
  select(Receptor, Treatment, p.value);shapiro.p

shapiro.s.p=spread(shapiro.p, Treatment, p.value);shapiro.s.p

bartlett.p <-
  df.bartlett.glance %>%
  select(Receptor, p.value);bartlett.p

ttest.p <-
  df.ttest.glance %>%
  select(Receptor, p.value);ttest.p

wilcox.p <-
  df.wilcoxtest.glance %>%
  select(Receptor, p.value);wilcox.p

f.shapiro=rename(shapiro.s.p, s.t.p.value = Treat, s.v.p.value = Veh)
f.bartlett=rename(bartlett.p, b.p.value = p.value)
f.ttest=rename(ttest.p, t.p.value = p.value)
f.wilcox=rename(wilcox.p, w.p.value = p.value)

t.1=full_join(f.shapiro, f.bartlett, by=NULL);t.1
t.2=full_join(t.1, f.ttest, by=NULL);t.2
t.f=full_join(t.2, f.wilcox, by=NULL);t.f


write.csv(t.f, "orphandata.csv")
```

A.1.2 Code to plot receptor heat map (Figure 3, Panel A)

```
library(ggplot2)
library(scales)
df <- read.csv(file.choose(), header=TRUE); df

ggplot(df, aes(df$Receptor, df$Replicate))+ ## Arrange your data like this (i.e. columns with receptors and replicates, like the sample spreadsheet)
  geom_tile(aes(fill=df$Sig)) +
  theme_classic() +
  labs(x = "Receptor", y = "Replicate", fill="p-value") +
  theme(axis.text = element_text(size = 28)) +
  theme(axis.title = element_text(size = 36, face="bold")) +
  theme(legend.title = element_text(size = 28, face ="bold")) +
  theme(legend.text = element_text(size=30)) +
  theme(panel.border = element_rect(fill=NA)) +
  theme(strip.text.x = element_text(size = 32)) +
  scale_fill_gradientn(colours=c("#0c4085","white"),limits = c(0,1)) +
  scale_colour_continuous(expand=c(0,0),limit=c(0,1))+
  theme(axis.text.x = element_text(angle = 90, hjust = 1))
```